Quantum thermodynamics of solids by means of an effective potential

A. Cuccoli and A. Macchi
Dipartimento di Fisica dell'Università di Firenze, Largo Enrico Fermi 2, I-50125 Firenze, Italy

M. Neumann
Institut für Experimentalphysik, Universität Wien, Strudlhofgasse 4, A-1090 Wien, Austria

V. Tognetti
Dipartimento di Fisica dell'Università di Firenze, Largo Enrico Fermi 2, I-50125 Firenze, Italy

R. Vaia
Istituto di Elettronica Quantistica del Consiglio Nazionale delle Ricerche, Via Panciatichi 56/30, I-50127 Firenze, Italy
(Received 15 April 1991)

A theoretical approach is presented that allows reproduction of the thermodynamic properties of anharmonic solids with low quantum coupling, such as solid argon, over the entire temperature range. The properties of the quantum system are obtained from classical Monte Carlo simulations by means of an effective potential which is based on a variational method developed recently. This technique is tested against extensive path-integral Monte Carlo calculations on a Lennard-Jones model of solid argon, and excellent agreement is found. It is also shown that the Lennard-Jones potential, with parameters derived from gas-phase data, provides a very good description of argon in the solid state.

I. INTRODUCTION

The important role played by quantum effects on the thermodynamics of solids was already recognized very early in the development of quantum mechanics, and the basic phenomena could be explained by assuming that real crystals are arrays of point masses interacting through harmonic forces. Subsequently, most of the theoretical studies on the thermodynamics of solids were devoted to including the contributions of nonharmonic interactions into the quantum mechanical description. Although considerable progress has been made, this is still an open problem, however, since most of the theories adopting a direct quantum mechanical approach not only require the evaluation of rather complicated integrals in **k** space, but usually are also limited to a particular regime such as low-dimensional systems or the high- or low-temperature limit.[1]

The general availability of fast computers and the development of genuine quantum-mechanical Monte Carlo algorithms,[2] in particular the path-integral Monte Carlo (PIMC) technique,[3–5] have opened an alternative route to predicting thermodynamic properties of many-body systems theoretically, by means of direct numerical simulation. In practice, however, and when they are applied to realistic model systems, these methods are rather demanding in terms of computer time, especially at low temperatures where quantum effects become large.

An alternative that seems to suggest itself is the use of an effective potential, which reduces the quantum-mechanical problem to a classical simulation. Up to now, this approach was essentially restricted to gases and liquids at not too low temperatures: For example, the effective potential based on the Wigner expansion[6,7] is just the leading term in an asymptotic expansion of the density matrix in terms of either $\hbar$ or $\beta = 1/k_B T$,[8] which limits its applicability to almost classical systems.[9] On the other hand, the effective potential derived by Feynman[3] through a variational principle, is based on the quantum behavior of a free particle. Obviously, this is not an appropriate starting point for the solid. Therefore, Giachetti and Tognetti[10–12] introduced an improved variational method for nonharmonic many-body systems, by taking advantage of the fact that the low-temperature quantum character of solids is largely due to harmonic excitations, which can be treated exactly. (A similar treatment for the single-particle case has been proposed by Feynman and Kleinert.[13])

We have recently applied[14–16] this method to a linear chain of Lennard-Jones (LJ) particles, i.e., a one-dimensional model with realistic anharmonic interactions. It was found that the quantum Monte Carlo calculations by McGurn *et al.*[17] on the same model could be reproduced within just a few seconds on a personal computer. These results confirmed our feeling that this method might also be particularly useful in three dimensions, e.g., in simulations of the rare-gas solids whose interaction potential is reasonably well understood.[18] An application along these lines has in fact been reported very recently by Liu, Horton, and Cowley,[19] who studied a simple three-dimensional nearest-neighbor LJ model for solid argon. Although Liu, Horton, and Cowley could demonstrate the feasibility of three-dimensional calculations, and plausible results were obtained over the whole

temperature range, including the correct behavior in the high- or low-temperature limit, it remained unclear whether this method actually yields quantitatively useful results.

Therefore, in the present paper the problem is considered in greater depth, and several aspects are addressed: Firstly, although we, too, represent solid argon by an LJ model cut off beyond the nearest-neighbor distance, the long-range interactions are taken into account in a static approximation. This cutoff correction, which is common practice in condensed-matter simulations,[20] allows us to use the well-established LJ potential parameters for argon, which were determined from gas-phase data[21] and give a reasonable representation of the true pair potential. Secondly, in the calculation of the effective potential the true phonon curves for the fcc lattice, rather than the isotropic approximation of Ref. 19, are used.

In order to assess the validity of the present approach, the results of our Monte Carlo simulations with the effective potential (EPMC) were compared with a set of very extensive PIMC calculations for the same model system. In these calculations, rather high Trotter numbers were required to perform the extrapolation to the quantum-mechanical limit. However, bearing in mind that at low temperatures the system becomes increasingly harmonic, the simple action of adding the corresponding corrections from the harmonic model greatly facilitates the extrapolation procedure. This was particularly useful in the case of the specific heat.

Finally, we also present a comparison of our EPMC results with experimental data on solid argon. This is not meant to be another test—the LJ is not even the correct *pair* potential for real argon[18]—but it should demonstrate that realistic simulations of low-temperature solids have now become economical as well as feasible.

II. THE EFFECTIVE POTENTIAL

We consider a Bravais lattice of N identical atoms with mass m, interacting through a spherically symmetric pair potential $u(r)$. Its Hamiltonian is

$$H = \sum_{\boldsymbol{l}} \frac{m}{2} \dot{\mathbf{x}}_{\boldsymbol{l}}^{\,2} + V(\mathbf{X}) \ , \tag{1}$$

where

$$V(\mathbf{X}) = \frac{1}{2} \sum_{\boldsymbol{l}} \sum_{n} \sum_{\mathbf{d}_n} u(|\mathbf{x}_{\boldsymbol{l}+\mathbf{d}_n} - \mathbf{x}_{\boldsymbol{l}}|) \ . \tag{2}$$

Here, atoms are labeled by their equilibrium position $\boldsymbol{l}$; $\mathbf{x}_{\boldsymbol{l}}$ is the (instantaneous) position of the atom at lattice site $\boldsymbol{l}$, and the sum over $n = 1, 2, \ldots$ accounts for the successive shells of neighbors of atom $\boldsymbol{l}$, which, in equilibrium, are at relative positions $\mathbf{d}_n$.

The derivation of an effective potential, which takes the quantum effects into account, has been the subject of several papers.[11,14–16,22–24] We refer principally to Ref. 14, where the thermodynamics of a linear chain of atoms interacting through a pair potential like (2) was studied.

In order to approximate the partition function

$$Z = e^{-\beta F} = \int_{\mathbf{X}(0)=\mathbf{X}(\beta\hbar)} \mathcal{D}\mathbf{X}(u)\, e^{-S[\mathbf{X}(u)]} \tag{3}$$

best, where

$$S[\mathbf{X}(u)] = \frac{1}{\hbar} \int_0^{\beta\hbar} du \left(\sum_{\boldsymbol{l}} \frac{m}{2} \dot{\mathbf{x}}_{\boldsymbol{l}}^2(u) + V(\mathbf{X}(u)) \right) \ , \tag{4}$$

we introduce the nonlocal trial action

$$S_0[\mathbf{X}(u)] = \frac{1}{\hbar} \int_0^{\beta\hbar} du \left(\sum_{\boldsymbol{l}} \frac{m}{2} \dot{\mathbf{x}}_{\boldsymbol{l}}^2(u) + w(\overline{\mathbf{X}}) + \frac{m}{2} [\mathbf{X}(u) - \overline{\mathbf{X}}]^T \omega^2(\overline{\mathbf{X}}) [\mathbf{X}(u) - \overline{\mathbf{X}}] \right) , \tag{5}$$

containing as variational parameters the scalar $w(\overline{\mathbf{X}})$ and the frequency matrix $\omega^2(\overline{\mathbf{X}})$, which both depend on the average point of the path, $\overline{\mathbf{X}} = \overline{\mathbf{X}}[\mathbf{X}(u)] = (\beta\hbar)^{-1} \int_0^{\beta\hbar} \mathbf{X}(u)\, du$.

It is apparent that the trial action (5) is the best (exactly solvable) starting point for our problem, at least for low quantum coupling, since low-temperature solids can indeed be described in terms of quantum harmonic oscillators.

The variational parameters ω and w are determined by minimizing the right-hand-side (rhs) of the Jensen-Feynman inequality[25]

$$F \leq F_0 + T\langle S - S_0 \rangle_0 \ , \tag{6}$$

where F is the "true" free energy of the system, F_0 the free energy associated with the trial action S_0, and $\langle \cdots \rangle_0$ is the functional average calculated over the distribution of paths given by S_0.

The minimization with respect to w gives $\langle S - S_0 \rangle_0 = 0$, so that the best variational approximation to the free energy F is F_0 itself. The path integral for the trial action (5) can be evaluated exactly, leaving only a final integration over $\overline{\mathbf{X}}$, so that the calculation of the partition function is reduced to the classical-like configurational integral

$$Z \simeq \left(\frac{m}{2\pi\hbar^2\beta} \right)^{\frac{3}{2}N} \int e^{-\beta V_{\text{eff}}(\mathbf{X})} d\mathbf{X} \ , \tag{7}$$

where $V_{\text{eff}}(\mathbf{X})$ is the effective potential.

The explicit expressions for the variational parameters and the effective potential associated with model (2) can be obtained by generalizing those of Ref. 14 to a three-dimensional lattice. Basically, one has to replace the site indices i appearing in Ref. 14 by the pair $\boldsymbol{l}i$, where i now refers to the Cartesian components, while the indices k of the normal modes of vibration are replaced by the pair $\mathbf{k}\mu$, where μ denotes the polarization. The final result is

$$V_{\text{eff}}(\mathbf{X}) = w(\mathbf{X}) + \frac{1}{\beta} \sum_{\mathbf{k},\mu} \ln \frac{\sinh[f_{\mathbf{k}\mu}(\mathbf{X})]}{f_{\mathbf{k}\mu}(\mathbf{X})} \ , \tag{8}$$

with

$$w(\mathbf{X}) = \int V(\mathbf{X} + \underline{U}^T \boldsymbol{\eta}) \prod_{\mathbf{k},\mu} \frac{e^{-\eta_{\mathbf{k}\mu}^2/2\alpha_{\mathbf{k}\mu}(\mathbf{X})}}{\sqrt{2\pi\alpha_{\mathbf{k}\mu}(\mathbf{X})}} \, d\eta_{\mathbf{k}\mu} - \frac{m}{2} \sum_{\mathbf{k},\mu} \omega_{\mathbf{k}\mu}^2(\mathbf{X}) \, \alpha_{\mathbf{k}\mu}(\mathbf{X}) \ , \tag{9}$$

where

$$\alpha_{\mathbf{k}\mu}(\mathbf{X}) = \frac{\hbar}{2m\omega_{\mathbf{k}\mu}(\mathbf{X})} \left(\coth[f_{\mathbf{k}\mu}(\mathbf{X})] - \frac{1}{f_{\mathbf{k}\mu}(\mathbf{X})} \right) \ ,$$

$$f_{\mathbf{k}\mu}(\mathbf{X}) = \frac{\beta\hbar\omega_{\mathbf{k}\mu}(\mathbf{X})}{2} \ , \tag{10}$$

and $\omega_{\mathbf{k}\mu}^2(\mathbf{X})$ are the eigenvalues of the frequency matrix

$$\omega_{\mathbf{l}\mathbf{m},ij}^2(\mathbf{X}) = \frac{1}{m} \int \frac{\partial^2 V}{\partial x_{\mathbf{l}i} \partial x_{\mathbf{m}j}} (\mathbf{X} + \underline{U}^T \boldsymbol{\eta}) \times \prod_{\mathbf{k},\mu} \frac{e^{-\eta_{\mathbf{k}\mu}^2/2\alpha_{\mathbf{k}\mu}(\mathbf{X})}}{\sqrt{2\pi\alpha_{\mathbf{k}\mu}(\mathbf{X})}} \, d\eta_{\mathbf{k}\mu} \ , \tag{11}$$

which is diagonalized by the orthogonal matrix $\underline{U} = \underline{U}(\mathbf{X})$.

As is apparent from the previous formulas, the quantum character of the system enters into the effective potential in two ways: first of all, in the logarithmic term, which takes the full quantum behavior of the harmonic excitations into account, and secondly, in the broadening of the potential due to the (Gaussian) quantum fluctuations of the particle positions. In fact, $\alpha_{\mathbf{k}\mu}$ is just the pure quantum contribution to the (quadratic) fluctuations of the normal mode $\mathbf{k}\mu$.

As in previous applications of the improved variational method to many-body systems,[14,15,22–24] we limit ourselves, in the following, to the low coupling approximation (LCA) to the effective potential. Within this approach, the configuration dependence of $\underline{U}$, $\omega_{\mathbf{k}\mu}$ and $\alpha_{\mathbf{k}\mu}$ can be neglected, and the quadratic term appearing in the trial action (5) is simply the second-order expansion of the potential around the equilibrium configuration, so that its diagonalization reduces to the phonon problem for the actual lattice. It follows that the orthogonal matrix $\underline{U}$ is the product of the Fourier transformation matrix $A_{\mathbf{k}l}$ and the 3×3 polarization matrices $\epsilon_{\mu i}(\mathbf{k})$ defined by

$$\omega_{\mathbf{k}\mu}^2 \delta_{\mu\nu} = \sum_{i,j} \epsilon_{\mu i}(\mathbf{k}) \, \omega_{\mathbf{k},ij}^2 \, \epsilon_{\nu j}(\mathbf{k}) \ , \tag{12}$$

where $\omega_{\mathbf{k}\mu}$ are the phonon frequencies of the lattice, and, using the subscripts ij to denote the derivatives of $u(|\mathbf{x}|)$,

$$m \, \omega_{\mathbf{k},ij}^2 = \sum_n \sum_{\mathbf{d}_n} u_{ij}(d_n) \, 2\sin^2 \left(\frac{\mathbf{k} \cdot \mathbf{d}_n}{2} \right) \ . \tag{13}$$

The LCA effective potential at temperature T can now be written as

$$V_{\text{eff}}(\mathbf{X}) = \frac{1}{2} \sum_{\boldsymbol{l}} \sum_n \sum_{\mathbf{d}_n} \left(u(|\mathbf{x}_{\boldsymbol{l}+\mathbf{d}_n} - x_{\boldsymbol{l}}|) + \frac{1}{2} \left[u_{ij}(|\mathbf{x}_{\boldsymbol{l}+\mathbf{d}_n} - \mathbf{x}_{\boldsymbol{l}}|) - u_{ij}(d_n) \right] D_{n,ij} \right) + \frac{1}{\beta} \sum_{\mathbf{k},\mu} \ln \frac{\sinh f_{\mathbf{k}\mu}}{f_{\mathbf{k}\mu}} \ , \tag{14}$$

where

$$D_{n,ij} = \sum_{\mathbf{k},\mu} \left(A_{\mathbf{k},\boldsymbol{l}+\mathbf{d}_n} - A_{\mathbf{k}\boldsymbol{l}} \right)^2 \epsilon_{\mu i}(\mathbf{k}) \epsilon_{\mu j}(\mathbf{k}) \, \alpha_{\mathbf{k}\mu} \tag{15}$$

is the tensor of the pure quantum fluctuations of the displacement between atom $\boldsymbol{l}$ and its nth-shell neighbors in the harmonic approximation. Due to the symmetry properties of the lattice, the D_n's are independent of $\boldsymbol{l}$ and of the direction of $\mathbf{d}_n$, so there is only one tensor D_n for each shell of neighbors.

Keeping in mind that the terms in (14) proportional to D_n account for the effects of the quantum fluctuations, we can neglect the fluctuations of the angular dependence of the vectors connecting each atom with its neighbors within the LCA. In this way the central character of the interaction potential is preserved in V_{eff}, which can finally be written

$$V_{\text{eff}}(\mathbf{X}) = \frac{1}{2} \sum_{\boldsymbol{l}} \sum_n \sum_{\mathbf{d}_n} u_n^{(\text{eff})}(|\mathbf{x}_{\boldsymbol{l}+\mathbf{d}_n} - x_{\boldsymbol{l}}|) + \frac{1}{\beta} \sum_{\mathbf{k},\mu} \ln \frac{\sinh f_{\mathbf{k}\mu}}{f_{\mathbf{k}\mu}} \ , \tag{16}$$

where

$$u_n^{(\text{eff})}(r) = u(r) + \frac{1}{2}[u''(r) - u''(d_n)] D_n^L + \frac{1}{2} \left(\frac{u'(r)}{r} - \frac{u'(d_n)}{d_n} \right) D_n^T \ , \tag{17}$$

and D_n^L and D_n^T are the longitudinal and transverse projections of the tensor $D_{n,ij}$:

$$D_n^L = \sum_{i,j} \frac{d_{n,i} d_{n,j}}{d_n^2} \, D_{n,ij} \ ,$$

$$D_n^T = \sum_{i,j} \left(\delta_{ij} - \frac{d_{n,i} d_{n,j}}{d_n^2} \right) D_{n,ij} \ . \tag{18}$$

III. MODEL POTENTIAL AND MONTE CARLO CALCULATIONS

In order to benchmark the effective potential approach, we have carried out a number of Monte Carlo simulations for a simple model of solid argon. In all these calculations, the interaction potential was assumed to be pairwise additive and given by the Lennard-Jones form

$$u(r) = 4\varepsilon \left[\left(\frac{\sigma}{r} \right)^{12} - \left(\frac{\sigma}{r} \right)^6 \right] , \tag{19}$$

with $\varepsilon/k_B = 119.8$ K and $\sigma = 3.405$ Å. The quantum

behavior of the model is characterized by the coupling parameter $\lambda = \hbar\Omega/\varepsilon$, with $\Omega^2 = u''(\sqrt[6]{2}\sigma)/m$, which turns out to be small ($\lambda = 0.224$) for argon.[14]

It is well known that (19) is not the true pair interaction for argon, and more refined potentials have been proposed in the literature.[26] A theoretically based, quantitative description of the dense phases even requires the inclusion of irreducible three-body forces.[27] Nevertheless, the LJ model appears to be a very efficient *effective* pair potential, giving virtually quantitative results both in the low- and high-density range,[28] which is sufficient for our present purposes.

The ε and σ values quoted above are those determined from high-temperature gas phase data,[21] but also the phonon dispersion curves deduced from them are in excellent agreement with experiment.[29] Therefore, we prefer to retain these "natural" values also in the solid phase, and in Sec. IV it will be shown that the gas-phase parameters in fact permit a consistently accurate description of argon all the way down into the solid phase.

With this model potential a number of Monte Carlo calculations, including classical Monte Carlo (MC) simulations, classical simulations with the effective quantum-mechanical potential (EPMC), and path-integral Monte Carlo (PIMC) simulations, were performed for a selection of thermodynamic states. In all these calculations, the sample consisted of a fcc lattice of $N = 108$ atoms enclosed in a cubical box to which periodic boundary conditions were applied. Only nearest-neighbor interactions were dynamically taken into account; the contributions from more distant neighbors were approximated by the values appropriate for an infinite static fcc lattice. The corresponding correction terms to the potential energy and pressure are of the order of -2.5 kJ/mol and -2000 atm, respectively. With this simple procedure, excellent agreement with the experimental equation of state of solid argon is obtained, and the use of unphysical parameter values is avoided.[19] Sample calculations allowing for dynamical interactions up to the second-neighbor shell were performed but showed no significant differences in the numerical results.

All Monte Carlo simulations were based on the Metropolis algorithm and single-particle moves.[20] The maximum displacement was chosen such as to lead to an acceptance ratio of 10–50 % of the trial moves. Each run was started from a perfect fcc lattice at the appropriate density and equilibrated for at least 5000 passes (trial moves per particle). Depending on the specific Monte Carlo technique, averages were then accumulated every fifth configuration for another 50 000–500 000 passes.

In the classical Monte Carlo simulations each run consisted of 50 000 passes and was analyzed in the usual manner.[20] In the simulations with the effective potential (EPMC), which consisted of 75 000 passes each, the time required to calculate the effective potential is entirely negligible compared to the total simulation time. Since the effective potential depends on temperature as well as on density (and has to be recalculated for each thermodynamic state), it is not possible to use the standard expressions[20] for the calculation of thermodynamic quantities such as total energy E, pressure p, and specific heat C_V. Rather, one has to re-derive the microscopic expressions to be averaged, by starting from the thermodynamic relationships $E = \partial(\beta F)/\partial\beta$, $p = -\partial F/\partial V$, and $C_V = -k_B\beta^2\partial^2(\beta F)/\partial\beta^2$ and taking the dependence of the renormalization parameters $D^{L,T}$ and the logarithmic term in V_{eff} on β and the equilibrium lattice spacing explicitly into account.

In the PIMC simulations, the primitive algorithm was used.[4,20] A trial move consisted of a random displacement of the "center of mass" of the classical ring polymer which, in the limit $P \to \infty$, is equivalent to the quantum-mechanical particle, combined with a set of "intramolecular coordinates" sampled from the free-particle density matrix. The Trotter number P—the number of beads on the ring polymers—was varied between 4 and 64, and each run consisted of 500 000 passes after equilibration. The "crude" energy estimator[20,30,31] was used, and the specific heat was calculated through a fluctuation formula derived in the manner outlined for EPMC above.

TABLE I. Thermodynamic properties of solid LJ argon at T=0.083 47 (10 K), ρ=1.0533. Here and in the following tables, all quantities are given in reduced units. ρ is the number density, K the kinetic energy, U the potential energy, E the total energy, p the pressure, and C_V the specific heat. The columns labeled "+HC" were obtained by adding the harmonic correction to the raw PIMC data in the preceding column. The extrapolated values are listed as "$P = \infty$." (See the text.)

	K/N	U/N	E/N		p		C_V/N	
				MC				
	0.1252		−8.3200		−1.577		2.96 ±0.02	
				PIMC				
				+HC		+HC		+HC
P=4	0.3045	−8.2770	−7.9726	−7.8033	−0.5059	0.0362	3.22 ±0.01	0.52
8	0.3700	−8.2192	−7.8491	−7.7913	−0.1391	0.0467	1.78 ±0.03	0.57
16	0.3982	−8.1958	−7.7976	−7.7816	0.0101	0.0617	0.89 ±0.12	0.52
32	0.4063	−8.1886	−7.7823	−7.7782	0.0558	0.0691	0.66 ±0.13	0.53
64	0.4087	−8.1868	−7.7781	−7.7771	0.0676	0.0709	0.19 ±0.42	0.17
∞	0.410	−8.185	−7.774	−7.775	0.077	0.076	0.56	0.54
				EPMC				
			−7.7995		0.052		0.50 ±0.02	

IV. RESULTS AND DISCUSSION

The results of our calculations are reported in Tables I–V and Figs. 1–6. Unless stated otherwise, all quantities are given in the usual dimensionless form, by reducing them with respect to the parameters of the LJ potential. Thus, energies are measured in units of ε, pressures in units of ε/σ^3, etc. On an absolute scale these energy and pressure units correspond to 0.9961 kJ/mol and 413.5 atm, respectively.

A. Consistency with PIMC calculations

Since our primary goal was to establish the validity of the EPMC approach by comparing the results to accurate quantum-mechanical calculations, we have carried out an extensive set of parallel MC, EPMC, and PIMC simulations at four selected thermodynamic states of the zero-pressure solid. The temperatures selected correspond to 10, 20, 40, and 60 K, and the densities were taken from the experimental work of Peterson, Batchelder, and Simmons[32] (see also Ref. 33). The results of these simulations are presented in Tables I–IV. With the exception of the specific heat, the statistical uncertainty is indicated by the number of decimal places given. The unlabeled columns in the PIMC sections contain the raw data from the simulations at finite Trotter number P; those marked "+HC" include the simple *ad hoc* correction decribed below.

Since the PIMC results had to be extrapolated to $P \to \infty$, generally separate runs were done with P=4, 8, 16, and 32. When plotted as a function of $1/P$, the finite-P values usually fall on a smooth curve, which tends to a rather well-defined limit as $1/P \to 0$. This is shown for the kinetic energy K, total energy E, pressure p, and specific heat C_V, all at 10 K, in Figs. 1–4. (Error bars: These error bars were obtained by breaking each run into five segments of 100 000 passes each and calculating the standard error of the mean.) In this way the energies and pressures may be extrapolated by fitting a parabola through the points with $P > 4$. (At 60 K all points were included in the fit.) These extrapolated values are also included in Tables I–IV ("$P = \infty$").

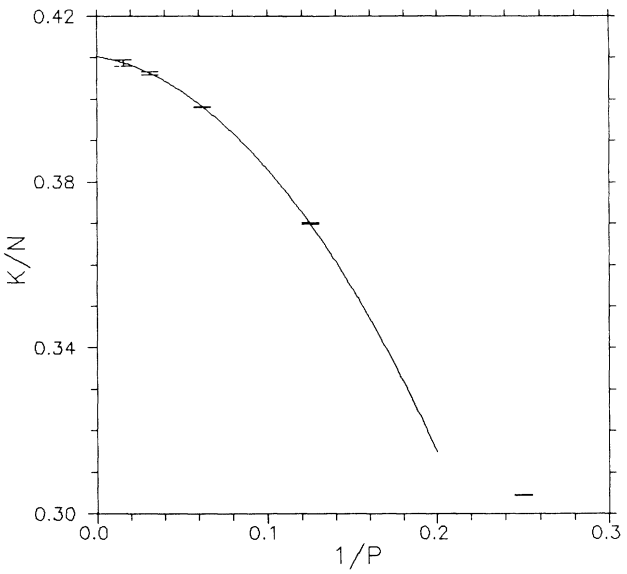

FIG. 1. Kinetic energy K of solid LJ argon at T=0.083 47 (10 K), ρ=1.0533 (reduced units). Error bars: PIMC calculations at Trotter number P=4, 8, 16, 32, and 64; solid line: quadratic fit through points with $P \geq 8$.

For the specific heat, however, the uncertainties are so large that no useful results could be obtained at a higher Trotter number. For instance, the values for $P = 16$ at 20 and 60 K are clearly outlying, given the measured error bars. This is due to our use of a fluctuation formula for C_V, which generally converges rather slowly. By hindsight, it might have been more economical to calculate C_V by numerically differentiating the total energy E, for which very accurate results may be obtained. We have verified this by performing two additional calculations, at 19 and 21 K, with $P = 16$. When calculated from the difference in total energy, $C_V/N = 1.52 \pm 0.01$, which

TABLE II. Thermodynamic properties of solid LJ argon at T=0.1669 (20 K), ρ=1.0499. Symbols as in Table I.

	K/N	U/N	E/N		p		C_V/N	
				MC				
	0.2504		−8.0690		−0.997		2.91 ±0.02	
				PIMC				
				+HC		+HC		+HC
P=4	0.4076	−8.1781	−7.7705	−7.7144	−0.1152	0.0650	2.12 ±0.02	1.55
8	0.4349	−8.1552	−7.7204	−7.7048	0.0302	0.0802	1.66 ±0.03	1.48
16	0.4439	−8.1484	−7.7045	−7.7011	0.0739	0.0868	1.35 ±0.08 [a]	1.30
32	0.4456	−8.1466	−7.7011	−7.7001	0.0852	0.0884	1.60 ±0.19	1.59
∞	0.446	−8.146	−7.700	−7.699	0.089	0.093	1.52	1.54
				EPMC				
			−7.7136		0.088		1.53 ±0.02	

[a] A more accurate value, obtained from the total energy difference between separate runs at 19 and 21 K, is 1.52 ± 0.01 (see the text).

TABLE III. Thermodynamic properties of solid LJ argon at T=0.3339 (40 K), ρ=1.0325. Symbols as in Table I.

	K/N	U/N	E/N		p		C_V/N	
				MC				
	0.5008		−7.5430		−0.425		2.82 ±0.02	
				PIMC				
				+HC		+HC		+HC
P=4	0.5988	−7.9627	−7.3639	−7.3481	0.0520	0.1023	2.47 ±0.02	2.40
6	0.6059	−7.9575	−7.3516	−7.3445	0.0846	0.1174	2.46 ±0.05	2.43
8	0.6083	−7.9557	−7.3474	−7.3434	0.0960	0.1089	2.37 ±0.03	2.35
12	0.6091	−7.9545	−7.3454	−7.3436	0.1034	0.1092	2.43 ±0.08	2.42
16	0.6098	−7.9539	−7.3441	−7.3431	0.1067	0.1099	2.34 ±0.08	2.33
32	0.6108	−7.9535	−7.3427	−7.3424	0.1097	0.1105	2.26 ±0.36	2.26
∞	0.611	−7.953	−7.342	−7.343	0.111	0.110	2.33	2.36
				EPMC				
			−7.3471		0.109		2.37 ±0.02	

appears to be "correct." The extrapolated PIMC values quoted for C_V in Tables I–IV were finally obtained by excluding obviously outlying values and fitting a low-order polynomial to be compatible with the general trend and scatter of the points (cf. Fig. 4). Clearly, these values are rather imprecise.

As can be seen from Tables I–IV and Figs. 1–4, quite large Trotter numbers are required to approach the quantum-mechanical limit. Since this is mainly due to the inability of the PIMC simulations to cope with the full quantum behavior of the harmonic excitations (the "primitive algorithm" used here is based on the free-particle density matrix), the following procedure was devised: The thermodynamic properties of the harmonic oscillator may be calculated analytically not only in the quantum-mechanical limit, but also for finite Trotter number P.[30,34] Thus, it is not difficult to evaluate these properties also for the harmonic approximation to the model under consideration (including its finite size and number of particles). Assuming that the nonharmonic part of the interactions is adequately sampled in PIMC simulations with finite P, we may then correct the simulation results by putting

$$A_\infty = A_P + (A_{H,\infty} - A_{H,P}) \ , \tag{20}$$

where A_P is the value of any property A obtained in a PIMC simulation with Trotter number P, and $A_{H,P}$ is the exact result for the harmonic model.

The efficacy of this simple trick may be appreciated from Figs. 2–4 (triangles). Even for low Trotter numbers the corrected PIMC results are now quite close to the quantum-mechanical limit, and the extrapolated values (using the same data points but lower-order polynomials) are in good agreement with the extrapolation of the bare PIMC results. This proved to be especially helpful in the case of the specific heat where, within the statistical limits, the corrected C_V values appear to be almost independent of P. The numerical values are listed in column "+HC" (harmonic correction) of Tables I–IV.

Taking the difficulties in obtaining "exact" PIMC results into account, the performance of the EPMC approach is impressive indeed. From Tables I–IV it is obvious that the EPMC simulations are generally in excellent agreement with the exact results. For the specific heat the EPMC results even appear to be more reliable than the PIMC values. This is particularly gratifying in the intermediate temperature range ($0.2 < T < 0.5$), where no other approximate theories are available. The EPMC approach is also much more efficient than PIMC: Since P loosely coupled copies of the system are being simu-

TABLE IV. Thermodynamic properties of solid LJ argon at T=0.5008 (60 K), ρ=1.0070. Symbols as in Table I.

	K/N	U/N	E/N		p		C_V/N	
				MC				
	0.7513		−6.9788		−0.209		2.80 ±0.02	
				PIMC				
				+HC		+HC		+HC
P=4	0.8178	−7.6818	−6.8640	−6.8565	0.0861	0.1100	2.63 ±0.03	2.61
8	0.8223	−7.6788	−6.8565	−6.8559	0.1046	0.1106	2.60 ±0.08	2.59
16	0.8235	−7.6783	−6.8548	−6.8533	0.1081	0.1096	2.84 ±0.05	2.84
32	0.8247	−7.6780	−6.8533	−6.8532	0.1105	0.1109	2.82 ±0.22	2.82
∞	0.825	−7.678	−6.853	−6.853	0.111	0.110	2.6	2.61
				EPMC				
			−6.8567		0.109		2.59 ±0.02	

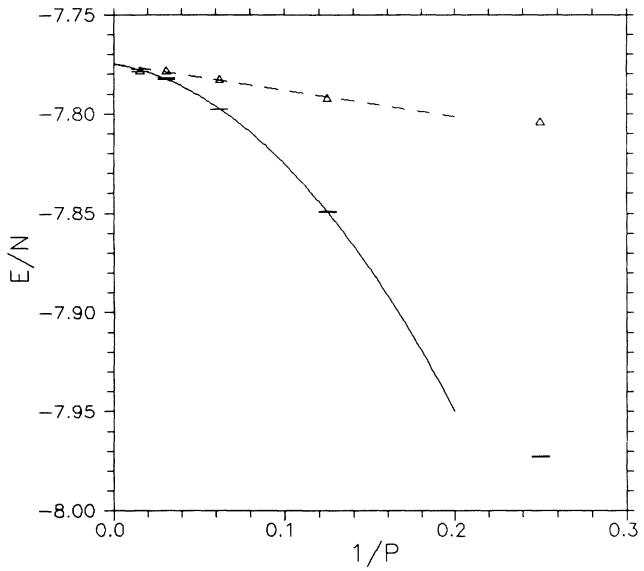

FIG. 2. Total energy E of solid LJ argon at T=0.083 47 (10 K), ρ=1.0533 vs inverse Trotter number P. Error bars: raw PIMC data; triangles: HC-corrected PIMC data (see the text); solid and dashed lines: quadratic (linear) fit through points with $P \geq 8$.

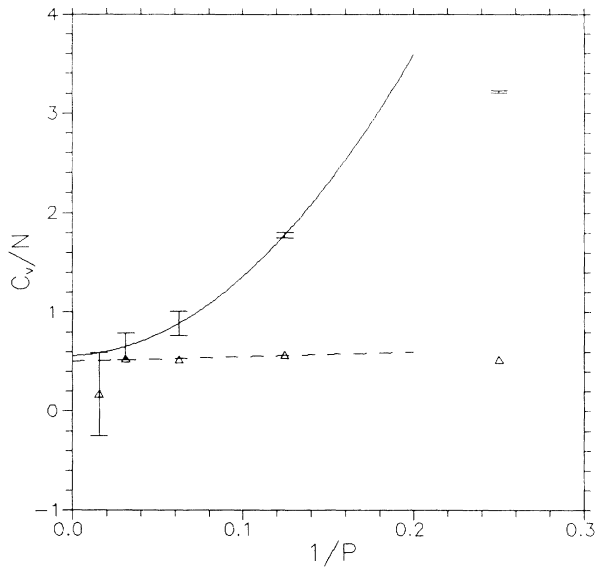

FIG. 4. Specific heat C_V of solid LJ argon at T=0.083 47 (10 K), ρ=1.0533. Symbols as in Fig. 2, except that also P=64 was excluded from the fit.

lated, a single PIMC calculation at Trotter number P is about P times slower than the corresponding EPMC simulation, and if a series of PIMC runs is required to extrapolate to $P \rightarrow \infty$, EPMC may be by one or two orders of magnitude more efficient than PIMC.

B. Comparison with experimental results

Having established the superior performance of the effective potential approach—at least for a system like solid argon whose quantum coupling parameter is small—the path is now open to apply the new technique to more realistic simulations, in order to enable a quantitative comparison with experimental results. This might include the use of "true" two- and three-body potentials, extension of interactions to more distant neighbors, etc., but is beyond the scope of the present paper.

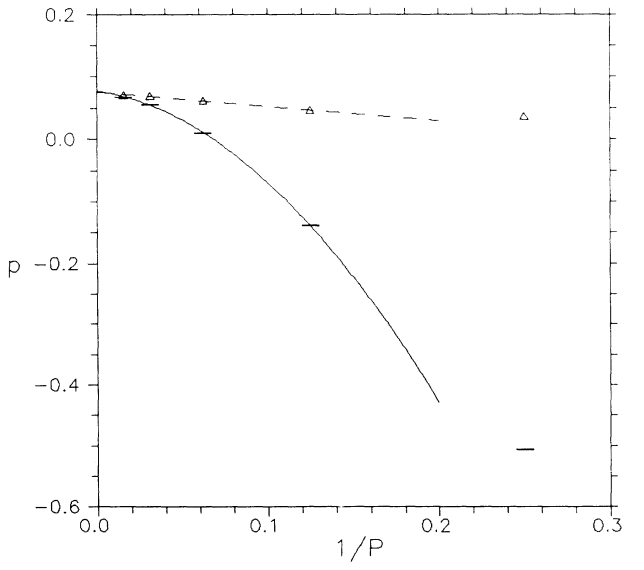

FIG. 3. Pressure p of solid LJ argon at T=0.083 47 (10 K), ρ=1.0533. Symbols as in Fig. 2.

In fact, it is surprising how well the equation of state of solid argon is reproduced even by the simple LJ model. When converted to absolute units, the pressures listed in Tables I–IV are of the order of 20–50 atm, which is normally considered by simulationists to be zero pressure. Thus, the LJ parameters obtained from the gas phase seem to yield excellent results not only in the dense liquid[28] but also in the low-pressure solid.

Bearing in mind that the particular way in which non-nearest-neighbor interactions were taken into account (static approximation) probably affects the calculated pressures by a larger amount than the net values quoted above, the agreement of the present results with the experimental equation of state must already be considered perfect. Nevertheless, and in order to demonstrate the facility with which EPMC calculations may be carried out, we have performed another series of MC-EPMC simulations to determine the zero-pressure (with a tolerance of ± 2 atm) densities of the model. The results for the density as well as for the specific heat are compared with the experimental data of Peterson, Batchelder, and Simmons[32] in Table V and Figs. 5 and 6.

In Fig. 5, the difference between the classical and quantum-mechanical results is seen to be predicted correctly, and the experimental densities are reproduced within a few tenths of a percent. Finally, in Fig. 6, the ability of EPMC calculations to predict the correct quantum-mechanical behavior of the specific heat is demonstrated convincingly, and the actual values are again in good agreement with the data on real argon.

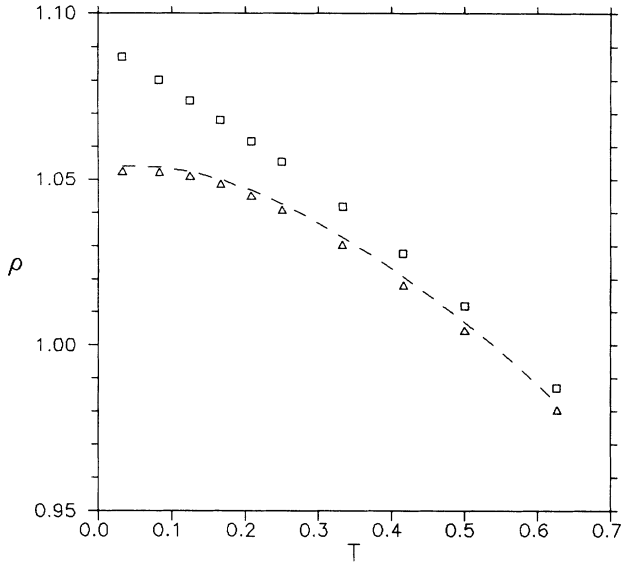

FIG. 5. Temperature dependence of the number density ρ for solid argon at zero pressure (reduced units). Squares and triangles: MC and EPMC calculations with the LJ model; dashed line: experimental data from Ref. 32.

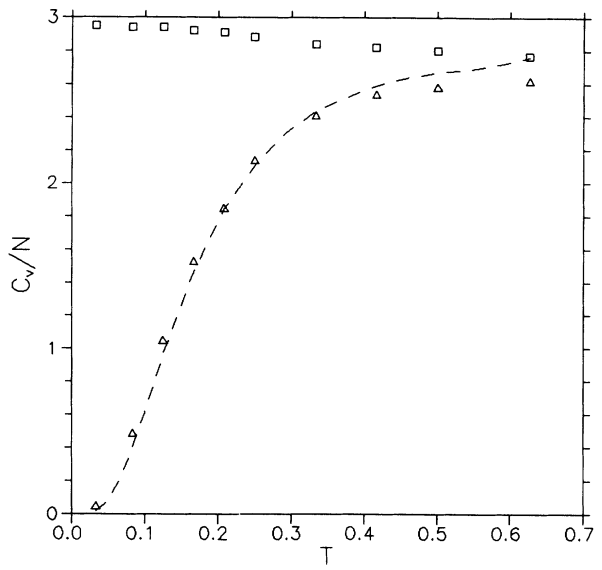

FIG. 6. Temperature dependence of the specific heat C_V for solid argon at zero pressure. Symbols as in Fig. 5.

V. CONCLUSION

The concept of describing a quantum-mechanical system by means of a classical system interacting through an effective potential may be traced back to the early work of Wigner.[6] When it can be effected, the complexity of the problem may be greatly reduced. This is true for theoretical work as well as for numerical simulations. In the latter case, substantial savings in terms of computer time may be achieved.

Whereas previous approaches were limited to almost classical, high-temperature systems, the effective potential derived via the improved variational method of Giachetti and Tognetti[10] seems to be ideally suited for theoretical calculations on anharmonic solids with low quantum coupling, since it is exact for the harmonic (i.e., low-temperature) model as well as in the high-temperature limit.

In the present paper we have shown that the present method is also quantitatively correct in the intermediate temperature range. This conclusion is based on a detailed comparison with path-integral Monte Carlo calculations on a Lennard-Jones model of solid argon. The EPMC results were found to be in excellent agreement with, or (in the case of the specific heat) even superior to, the PIMC simulations. We have also shown how low-Trotter-number PIMC data may be corrected by using a simple procedure based on the harmonic model. The corrected values are much closer (and easier to extrapolate) to the quantum mechanical limit.

On the experimental side, the simple LJ model, using the gas phase parameters, was found to give a very accurate description not only of the typical quantum be-

TABLE V. Density and specific heat of solid argon at zero pressure. Symbols as in Table I. In the simulations with the LJ model, the density was adjusted so that $p = 0 \pm 2$ atm. The experimental data were taken from Ref. 32.

	ρ			C_V/N		
T	MC	EPMC	Expt.	MC	EPMC	Expt.
0.0334 (4 K)	1.0869	1.0523	1.0540	2.95	0.05	0.021
0.0835 (10 K)	1.0801	1.0522	1.0537	2.94	0.49	0.396
0.1252 (15 K)	1.0739	1.0509	1.0525	2.94	1.05	0.963
0.1669 (20 K)	1.0678	1.0487	1.0499	2.92	1.53	1.462
0.2087 (25 K)	1.0615	1.0449	1.0467	2.91	1.85	1.840
0.2504 (30 K)	1.0552	1.0408	1.0426	2.88	2.14	2.104
0.3339 (40 K)	1.0416	1.0304	1.0325	2.84	2.41	2.436
0.4174 (50 K)	1.0276	1.0181	1.0206	2.82	2.54	2.591
0.5008 (60 K)	1.0120	1.0045	1.0070	2.80	2.58	2.669
0.6260 (75 K)	0.9871	0.9804	0.9826	2.77	2.62	2.759

havior of the specific heat, but also of the equation of state. This confirms once more its usefulness as an effective pair potential for argon over a wide density range, which is well known in the liquid state.[28]

In particular, the use of unphysical LJ parameter values[19] was avoided by accounting for long-range interactions in the static approximation, since only nearest-neighbor interactions were explicitly taken into account in the simulations. This was merely done for convenience and is not an inherent limitation of the EPMC method. The inclusion of non-nearest-neighbor interactions—test runs with second neighbors were performed, but did not show substantial modifications—as well as of more realistic potentials, is straightforward. Using the effective potential approach, such more detailed investigations have now become highly economical.

ACKNOWLEDGMENTS

One of us (M.N.) would like to acknowledge the hospitality of the Dipartimento di Fisica dell'Università di Firenze and of the Istituto di Elettronica Quantistica del CNR, during the early stage of this work. We have received support from the Bundesministerium für Wissenschaft und Forschung, Wien, in the form of unlimited access to their VAX-cluster (PIMC calculations), and from the Consorzio di Fisica della Materia (INFM). We also want to thank A.A. Maradudin, G.K. Horton, S. Liu, and M. Zoppi for useful discussions.

[1] A.A. Maradudin, P.A. Flinn, and R.A. Coldwell-Horsfall. Phys. Rev. B **40**, 2407 (1989).